Essence determines phenomenon: Assaying the material properties of biological condensates

Received for publication, November 16, 2021, and in revised form, February 16, 2022 Published, Papers in Press, March 2, 2022,
https://doi.org/10.1016/j.jbc.2022.101782

Zheng Wang[1,*], **Jizhong Lou**[2,3,*], **and Hong Zhang**[1,3,*]

From the [1]*National Laboratory of Biomacromolecules, and* [2]*Key Laboratory of RNA Biology, CAS Center for Excellence in Biomacromolecules, Institute of Biophysics, Chinese Academy of Sciences, Beijing, China;* [3]*College of Life Sciences, University of Chinese Academy of Sciences, Beijing, China*

Edited by Paul Fraser

Intracellular spaces are partitioned into separate compartments to ensure that numerous biochemical reactions and cellular functions take place in a spatiotemporally controlled manner. Biomacromolecules including proteins and RNAs undergo liquid–liquid phase separation and subsequent phase transition to form biological condensates with diverse material states. The material/physical properties of biological condensates are crucial for fulfilling their distinct physiological functions, and abnormal material properties can cause deleterious effects under pathological conditions. Here, we review recent studies showing the role of the material properties of biological condensates in their physiological functions. We also summarize several classic methods as well as newly emerging techniques for characterization and/or measurement of the material properties of biological condensates.

Eukaryotic cells govern the specificity and efficiency of their numerous intracellular processes, including their networks of biomolecular interactions, *via* distinct mechanisms. Membrane-enclosed organelles such as the endoplasmic reticulum (ER), mitochondria, and endosomal compartments ensure that diverse molecular pathways and biochemical reactions occur in stably maintained compartments in eukaryotic cells. Membrane-less compartments, such as stress granules (SGs), P-bodies, the nucleolus, and nuclear speckles, provide more dynamic and tuneable platforms for compartmentalization of various intracellular processes (Fig. 1*A*) (1–3). Membrane-less compartments are also known as condensates, granules, bodies, speckles, clusters, and so on. Hereafter, we will use the collective term "biological condensates" unless we describe a specialized compartment.

Phase separation and phase transition

Numerous biological condensates are known to assemble *via* phase separation, particularly liquid–liquid phase separation (LLPS). LLPS refers to a process in which a homogeneous solution system demixes into an inhomogeneous system containing at least two coexisting but spatially separate phases, both of which are in the liquid state (2, 3). Other types of phase separation such as liquid–solid phase separation have also been reported, for example, formation of SPD-5 assemblies in *Caenorhabditis elegans* and Rim4 fibrils in yeast (4, 5). Biological condensates formed *via* LLPS may further undergo phase transition, a process during which biological condensates transition between different material states. This endows them with distinct material/physical properties, which are tightly associated with their biological functions and intracellular fates in organisms (Fig. 1) (6, 7). This will be discussed in the sections below.

Phase-separated liquid condensates are highly mobile and dynamic. The constituent molecules diffuse readily and exchange with the surrounding environment (6, 7). However, biological condensates with liquid properties are thermodynamically metastable both in living cells and under experimental conditions *in vitro*. Newly formed liquid condensates may undergo phase transition with time *in vitro*: they gradually change into more stable and less dynamic states, such as hydrogels, liquid crystals, and amyloid-like fibrils (6–8). Phase transition of biological condensates into other states also occurs in living cells under both physiological and pathological conditions. However, numerous biological condensates maintain their liquid-like properties in organisms *via* various mechanisms, such as by assistance from the chaperone system in an ATP-dependent manner (7–9). Phase separation and transition of biological condensates can be influenced by various factors and conditions, which change the strength or valency of intermolecular interactions, such as temperature, pH, ionic strength, osmotic pressure, mechanical force, the composition and concentration of components, and various posttranslational modifications (7–9). Alteration of these factors and/or conditions may also modulate the material properties of the biological condensates. This allows the condensates to fulfill their distinct functions in various dynamic biological pathways and facilitates a timely response and adaptation to the complex and capricious external environment (6–9).

Driving forces for assembly of biological condensates

Biomacromolecules, including proteins, RNAs, DNAs, lipids, and polysaccharides, interact with each other *via* intermolecular forces. The electromagnetic force, which is

* For correspondence: Hong Zhang, hongzhang@ibp.ac.cn; Jizhong Lou, jlou@ibp.ac.cn; Zheng Wang, wz1103@ibp.ac.cn.

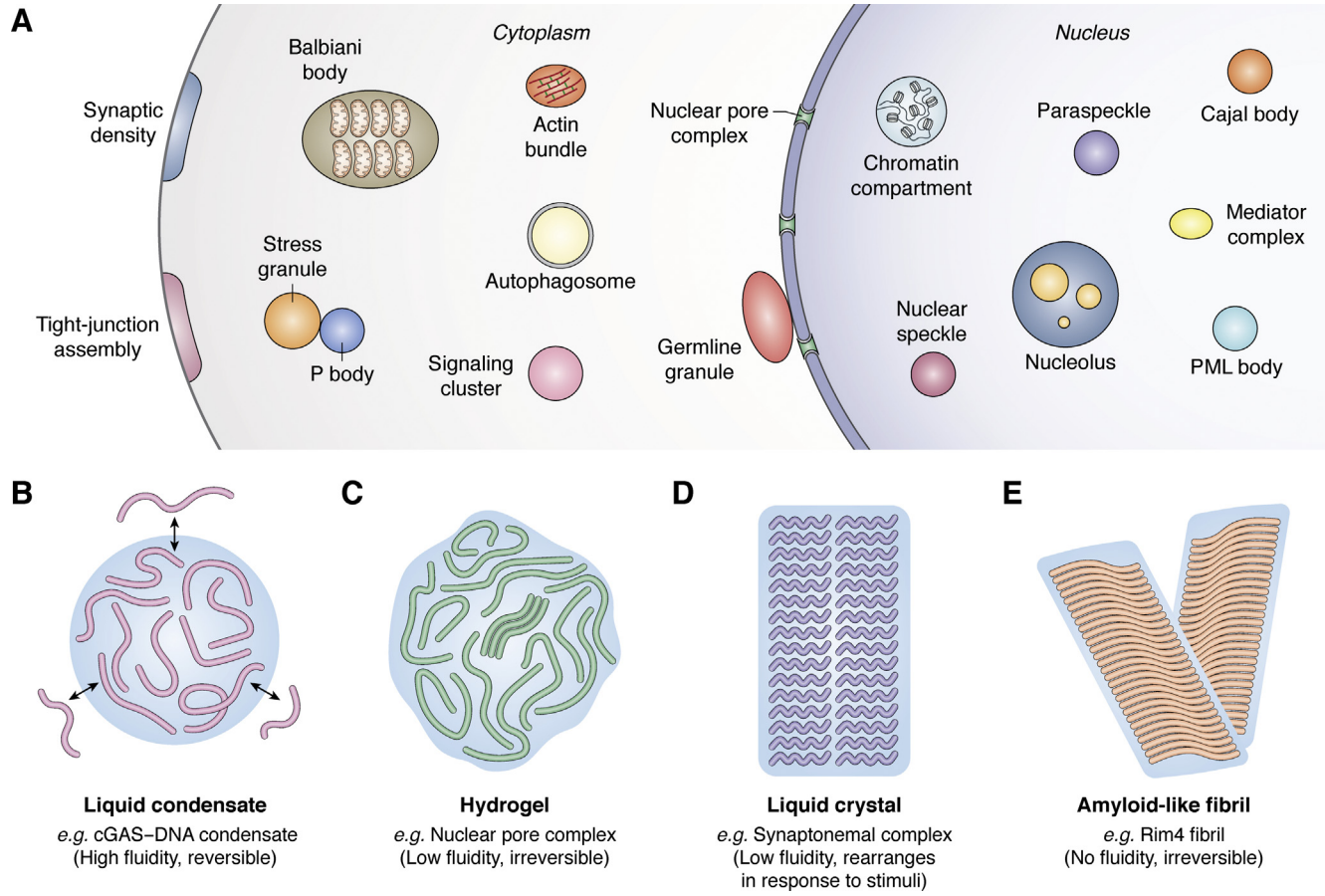

Figure 1. Biological condensates possess distinct material states. *A*, various biological condensates are assembled in eukaryotic cells and also at the cell–cell junctions. Many biological condensates, such as Balbiani bodies, germline granules, and synaptic densities, are formed only in specific cell types. *B*, biological condensates with liquid properties are highly dynamic and reversibly assembled. The biomolecules inside liquid condensates have high fluidity and can exchange with the surrounding environment. *C*, biological condensates resembling hydrogels are weakly dynamic and generally irreversibly assembled. Sometimes, hydrogels can be partially dissolved under certain conditions. For example, yeast Pab1 forms nondynamic gel-like condensates in response to heat stress, which can disassemble spontaneously when stress disappears (78, 115); several ATPase proteins can assist the disassembly to achieve the dynamic regulation of gel-like structures in living cells (116). The fluidity inside a hydrogel is very low, and the interior components undergo only limited exchange with the surroundings. *D*, some biological condensates consist of liquid crystal-like assemblies, in which the biomolecules are positioned in ordered arrangements. The components inside liquid-crystal structures have limited mobility under normal conditions, but rearrange in response to stimuli. *E*, solid-like biological condensates, such as amyloid-like fibrils, have no fluidity and are irreversibly assembled. The components inside solid-like structures are not mobile and cannot exchange with the surroundings.

derived from the electric fields generated by charge–charge interactions and magnetic fields induced by the movement of charged particles, includes the electrostatic force and van der Waals force, which underlie the most important interactions among biomolecules in biological systems. The electromagnetic forces between ions (such as glutamate (E) and lysine (K)) and polar molecules (such as serine (S) and threonine (T)) with permanent dipole moments are very strong, whereas the electromagnetic forces between nonpolar molecules (such as leucine (L) and valine (V)) are weak. Most proteins are polar in part and nonpolar on the whole. Gravity may also play a role for large complexes, organelles, or cells as a whole. The gravitational effect of individual biomolecules is negligible compared with the electromagnetic interactions and the entropy effect, while for larger condensates, gravity may need to be considered to understand their full properties. In this review, we mainly focus on the electromagnetic and entropic interaction aspects of the biological condensates.

Intermolecular interactions between biomacromolecules dissolved in aqueous solution at physiological conditions are influenced by multiple factors. Water condenses *via* the formation of hydrogen bonds, which have partial characteristics of both electromagnetic forces and covalent bonds. A protein dispersed in aqueous solution contacts water molecules and consequently disrupts the hydrogen bonds between the water molecules. If the intermolecular interactions between the protein and water molecules are strong enough to disrupt the hydrogen bonds between water molecules, the protein particles dissolve; otherwise they aggregate by excluding the water molecules. This entropic effect drives protein oligomerization and/or aggregation and is known as hydrophobic interaction. Other solutes dissolved in the aqueous solution, such as ions (*e.g.*, Ca^{2+}, Mg^{2+}, Zn^{2+}, etc.) and small molecular compounds (*e.g.*, ATP) affect protein–water interactions, making the situation more complicated. In biochemical systems, there are many electromagnetic forces and hydrophobic interactions

among biomacromolecules, including the electrostatic interactions between charged residues, hydrophilic interactions between polar residues, π-π stacking between aromatic residues, cation-π stacking between positively charged and aromatic residues, hydrogen bonds, and van der Waals forces (10). Ultimately, the solubility of a protein in aqueous solution is determined by its interactions with water and other solute molecules.

Biomacromolecules are natural polymers similar to those in the field of polymer chemistry and soft matter physics. They are densely packed with sites that can interact with other macromolecules. The free energy of a system consisting of a mixture of macromolecules is minimized by balancing the electromagnetic interactions, which contribute to enthalpy, and the hydrophobic interactions, which arise from entropy. Thus, intermolecular multivalent weak interactions may drive phase separation of dissolved biomacromolecules in aqueous solutions to form biological condensates (11). The multivalent weak intermolecular interactions that drive phase separation typically occur between intrinsically disordered regions (IDRs), low complexity regions (LCRs), modular protein domains, and nucleic acids such as RNAs (8). An IDR is a polypeptide region lacking a stable tertiary structure and usually exhibiting flexible and diverse conformations (7). In contrast to modular protein domains, the composition and distribution of residues in IDRs cannot satisfy the requirement for compact folding. Some IDRs have highly biased amino acid compositions, which are enriched in limited subsets of residues, such as glycine (G), glutamate (E), phenylalanine (F), and so forth. IDRs with this feature are also called LCRs (7). IDRs/LCRs can provide a rich source of binding sites for interacting biomolecules and serve as interaction platforms; thus, they are ideal scaffolds for the assembly of biological condensates. IDRs/LCRs are found in numerous proteins which undergo LLPS, and in many cases, the IDRs/LCRs are essential for LLPS. This implies that IDR/LCRs play a significant role in facilitating LLPS. Multivalent interactions between modular protein domains with compact folding may also trigger LLPS. These interactions may provide more specificity and strength for the assembly of biological condensates, such as postsynaptic density (PSD) condensates (12, 13). RNAs undergo LLPS alone in some cases, but more usually, they cophase separate with RNA-binding proteins in cells, to form condensates such as SGs, P-bodies, paraspeckles, and P granules (14–19). Notably, assembly and regulation of distinct biological condensates under physiological conditions are precise and highly specific in living cells. Dysregulation of these processes under certain conditions, such as pathological conditions, will elicit unexpected and/or nonspecific interactions, resulting in aberrant phase transition and altered material properties (7–9, 20, 21).

Relationship between the material properties and functions of biological condensates

The material state of biological condensates can be classified into liquid, hydrogel, liquid-crystal, crystal, glassy, amyloid-like fibril, and other solid-like states (6, 7, 22). Condensates can be more accurately characterized by their material/physical properties, such as concentration, diffusivity, viscosity, elasticity, interfacial tension, and so forth. Many lines of evidence reveal that the material properties of biological condensates are highly relevant to their physical functions and/or pathogenic roles.

Concentration and partition coefficient of components in biological condensates

Generally speaking, interactions between biomacromolecules and the activity of subsequent biological pathways are closely related to the concentration of the components. LLPS condenses biomolecules to enhance intermolecular interactions. Therefore, the concentration of the internal constituents is an important material characteristic of biological condensates. A biomacromolecule, when diluted in solution under a specific set of conditions, undergoes phase separation to form a condensate/dense phase upon reaching a certain concentration, which is known as the saturation concentration (C_{sat}) (23–26). A related parameter is the partition coefficient (K), the ratio of the concentration of a component in dense phase (C_{den}) to the concentration in dilute phase ($K=C_{den}/C_{sat}$) (27). Experimental evidence shows that in a simple binary phase separation system under a specific set of conditions, C_{sat} and K are both fixed on the basis of the underlying physics of LLPS (13, 23). An implication of the fixed C_{sat}, C_{den}, and K under physiological conditions is that condensate formation can passively buffer the cellular "noises" caused by fluctuation of the concentration of biomacromolecules (Fig. 2*A*) (23–27). Fluctuations of the concentration of proteins and RNAs may have a negative impact on a range of cellular processes. Formation of biological condensates and the consequent intrinsic concentration effects, therefore, provide a solution to the problem of noise, although there are also other mechanisms to resolve this predicament, such as bio-membranes and clustering (25, 28).

However, noise and the resulting individual variations in cells may also play pivotal roles in numerous biological processes, for example, development, evolution, and environmental adaptation (25, 29). In the case of *C. elegans* embryogenesis, P granules are specialized ribonucleoprotein (RNP) granules derived from the oocyte. They are assembled *via* LLPS in an RNA-dependent manner, and they asymmetrically segregate into daughter cells (30). P granules in germline blastomeres are preserved, while in somatic blastomeres, they are quickly disassembled and selectively removed (7, 31). The clearance of P granules in somatic blastomeres is dependent on the context of fluctuation of the C_{sat} required for LLPS of PGL-1/PGL-3 proteins, which are P granule components. Firstly, MEX-5, an RNA-binding protein, is asymmetrically distributed into the somatic blastomeres, where it competes with PGL-3 for mRNA. This increases the C_{sat} required for LLPS of PGL-3/-1, resulting in the disassembly of P granules in the somatic blastomeres (19). Secondly, after division, the somatic daughter cells express SEPA-1, a receptor protein that dramatically decreases the C_{sat} required for LLPS of PGL-1/-3. SEPA-1 expression thus selectively concentrates PGL-1/-3 into PGL granules for subsequent autophagic degradation (7, 31, 32). The composition-dependent

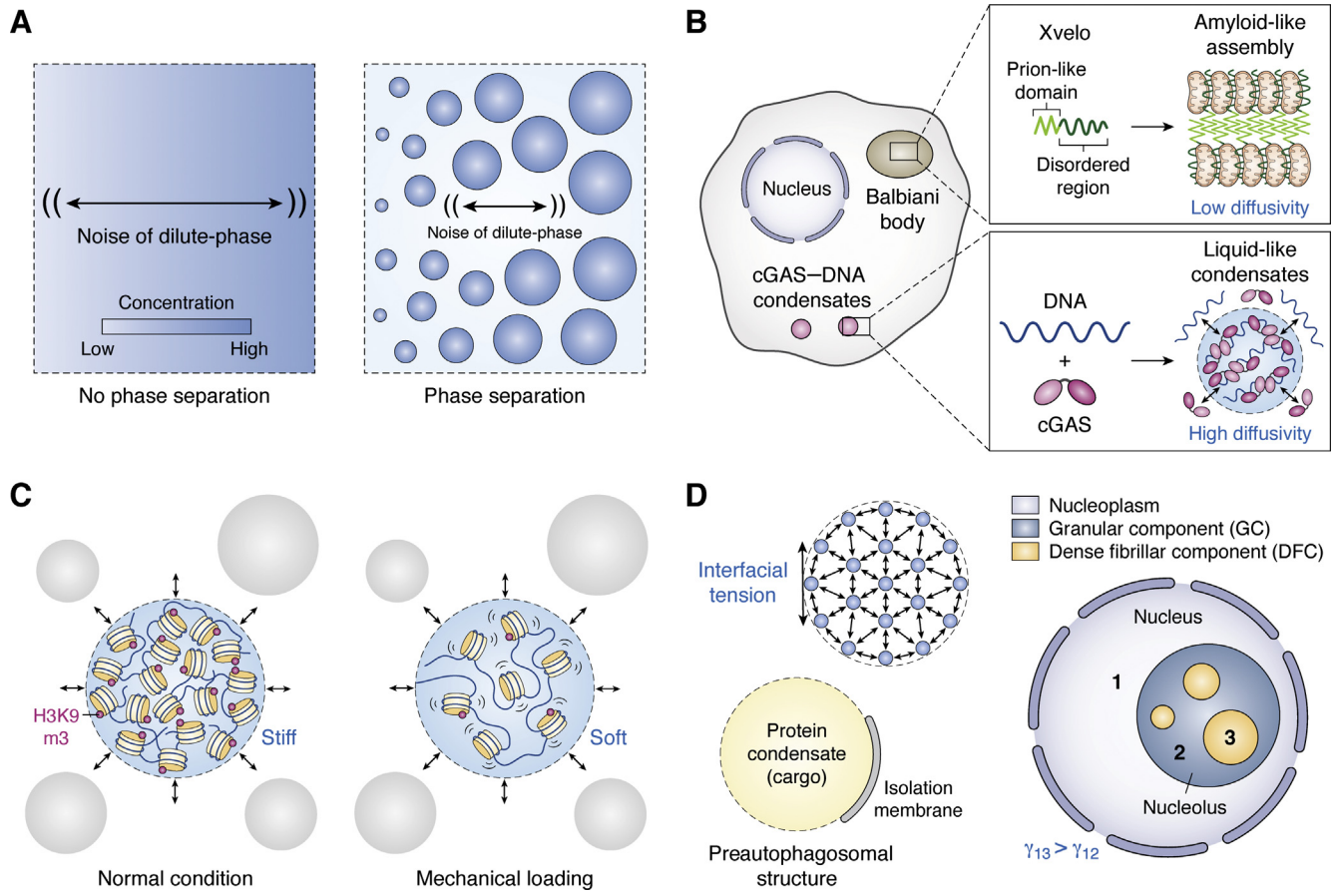

Figure 2. Material properties govern the physiological functions of biological condensates. *A*, cells buffer biological noises, caused by fluctuation of the biomolecular concentration, *via* phase separation. In cells without phase separation, the concentration of biomacromolecules may undergo drastic fluctuation, while in cells with phase separation, the concentrations in both the dilute phase and the dense phase are relatively stable in spite of fluctuations of the total amounts of biomacromolecules. *B*, the amyloid-like Balbiani body is inert and stable, which allows it to store dormancy cargos such as mitochondria in early oocytes. Liquid-like cyclic GMP–AMP synthase (cGAS)–DNA condensates are highly dynamic and possess mobile interior constituents, which make them suitable for efficient signal transduction. The Balbiani body is only assembled in early oocytes but is shown in the same cell as cGAS–DNA condensates for comparison purposes. *C*, heterochromatin compartments marked by histone H3 lysine 9 trimethylation (H3K9m3) are in the solid state and possess very high stiffness. These domains exclude multiple nuclear protein condensates and ensure the mechanical integrity of nuclei. Upon mechanical loading, the heterochromatic domains are demethylated and transition into less stiff compartments, in order to prevent mechanical damage to the genome. *D*, interfacial tension arises from the unbalanced forces on the molecules at the surface of biological condensates. Interfacial tension governs the interaction between immiscible phases. Examples include the formation of autophagosomes, in which liquid protein condensates (cargos) are engulfed by the double-membrane isolation membrane and the assembly of the multi-compartment nucleus. The actual architectures of these multi-phase assemblies in living cells are the result of minimizing the total interfacial energy. In the case of the nucleolus, the nucleoplasm has a higher interfacial tension with the dense fibrillar component (DFC) (γ13) than with the granular component (GC) (γ12), which results in engulfment of the DFC (phase 3) by the GC (phase 2).

adjustment to C_{sat} and K in heterotypic multicomponent LLPS systems may possibly occur widely in living cells. This mechanism may also passively buffer noise, since the variables in these systems are all linked. More constituents are buffered in multicomponent LLPS systems, and each one is buffered to a lesser extent than in condensates containing fewer components (24, 27). The concentration effect is important for phase separation to function in living cells.

Diffusivity and viscosity determine the liquidity of biological condensates

Diffusivity (*D*) of constituents in the dense phase reflects the liquidity of biological condensates and is also a direct parameter for characterizing the material state of biological condensates. It is often estimated by fluorescence recovery after photobleaching (FRAP) assays. The diffusivity of constituents in the dilute phase is usually very high and gradually decreases in the dense phase as the material states change from liquid to hydrogel and then to solid. Different condensates contain components with different diffusivities to fulfill distinct biological functions (Fig. 2*B*). For example, Balbiani bodies, which form solid-like condensates through the amyloid-like self-assembly of the disordered protein Xvelo, store RNA, mitochondria, and other organelles for dormancy in early oocytes (33). In contrast, biological condensates for signal transduction, such as LAT clusters, β-catenin destruction complexes, and cyclic GMP–AMP synthase–DNA condensates, are generally in highly dynamic liquid-like states (34–36). Dysregulation or aberrant changes of the diffusivity of constituents of biological condensates disrupt their physiological dynamics and functions. Such changes are associated with pathogenesis of various diseases, such as solidification of multiple RNP granules in various neurodegenerative diseases (37, 38). Of note, low diffusivity of constituents or solid-like

states of biological condensates does not always serve as an indicator of reduced activity. For example, the phosphatase activity of Herzog is activated upon amyloid-like assembly in developing *Drosophila* embryos (39).

The diffusivity of different components within the same condensates can differ greatly (40–43). Measuring the diffusivity of multiple individual components is therefore important for accurately characterizing the material states of biological condensates. The different diffusivity of distinct components can be important for their physiological functions. For example, in the case of nuclear pore complex barriers, which mediate nuclear-cytoplasmic shuttling, intrinsically disordered and phenylalanine/glycine-rich nucleoporins (FG-Nups) form hydrogel-like structures which exhibit very low liquidity to ensure the stability of the barriers; in contrast, the transported cargos are highly mobile so as to quickly traverse the nuclear pore complex barriers (44–47). Components within biological condensates have recently been divided into two qualitative classes, scaffolds and clients. The scaffolds are essential for formation of the condensates, while the clients, which are dispensable and variable, are recruited into the condensed structures by the scaffolds (3). Although they have distinct roles in the assembly of biological condensates, both scaffolds and clients can be involved in specifying the material properties of the condensates. For example, in *C. elegans* PGL granules, the diffusivity of the components within the condensates formed by the scaffold proteins PGL-1/-3 is very high. Upon recruitment of the client protein EPG-2 into PGL granules, the diffusivity of each component is significantly decreased (32). Moreover, the diffusivity of the same component may be different in distinct regions of a biological condensate. For example, SGs, a type of RNP granule that regulates the function and localization of mRNA under various stress conditions, adopt a "core-shell" structure for assembly in response to stress stimuli. The stable cores and dynamic shells contain different material states and differ in liquidity (48, 49).

In addition to diffusivity, viscosity (η) is also used to describe the fluidity of biological condensates. Viscosity reflects the resistance of a fluid to flow. It is usually negatively correlated with diffusivity and can be roughly estimated from the diffusivity of a certain component in a biological condensate *via* the Stokes-Einstein equation (50). Diffusivity can be considered to reflect the microscopic behaviors of components, whereas viscosity reflects the macroscopic property of the biological condensates. Liquid condensates have lower viscosity, while gel-like condensates have higher viscosity.

Elasticity and stiffness endow biological condensates with mechanical stability

Elasticity reflects the ability of solid materials to return to their original shape after deformation and compression upon mechanical loading. It can be quantitatively characterized as the elastic modulus (*E*). Elasticity is a property of materials but not objects. A material refers to physical matter such as wood, steel, and plastic that constitutes objects. An object possesses a distinct boundary with its surrounding environment(s). In the case of biological condensates, a phase-separated protein droplet with a specific size, density, and boundary is made of a liquid-like material (*i.e.*, a concentrated solution of proteins or other biomolecules). The deformation part of the elastic modulus is also known as Young's modulus. However, Young's modulus does not apply to liquid materials, since they do not have fixed shapes and easily flow upon loading. Therefore, the elasticity described in the field of biological phase separation is the apparent elasticity, which intrinsically reflects the stiffness (k) of the studied biological condensates. The apparent elasticity/stiffness are largely correlated with the shape, size, interface conditions, and other factors of the biological condensates. Apparent elasticity/stiffness are properties of objects but not materials. For biological condensates with liquid properties, the apparent elasticity/stiffness is largely determined by their interfacial tension, which will be discussed in the next section.

Elasticity/stiffness of biological condensates is important for the architectural integrity of many subcellular structures. For example, the expanded multivalent protein–protein network increases the stiffness of PSD condensates to ensure PSD assembly for establishment of the synapse in neurons (13). Dynamic modulation of the stiffness of heterochromatin, which undergoes LLPS to form highly elastic condensates, maintains the integrity of the nucleus (Fig. 2*C*) (43, 51–53). The rigid heterochromatin condensates marked by histone H3 lysine 9 trimethylation (H3K9m3) exclude multiple nuclear protein condensates to facilitate nuclear compartmentalization and to ensure the mechanical strength and sensitivity of the nucleus (51, 52). When cells are subjected to mechanical force, these condensates are quickly demethylated and transition into less stiff euchromatin, thus softening the nucleus to protect the genome from mechanical stress-induced damage (53).

Interfacial tension governs the surface behaviors of biological condensates

Two immiscible phases in contact generate an interfacial boundary. Statistically, molecules inside a bulk phase equally attract the same neighboring molecules in all directions, resulting in a net force of zero, while molecules at the surface are in a different situation. These molecules are strongly attracted to similar molecules in the bulk phase, while also undergoing weak interactions with different molecules from the other phase. Therefore, the surface molecules experience a net force toward the interior of the bulk phase and have a tendency to move toward the bulk phase to minimize the surface area. The force along the surface per unit length is known as interfacial tension (γ), or surface tension when the contacting phase is air or a vacuum (Fig. 2*D*, left top). At a liquid–liquid interface, interfacial tension is equivalent to interfacial energy, the work required to enlarge the surface per unit area. The free energy of the surface molecules is also higher than those in the bulk phase. The direction of interfacial tension is tangential to the surface.

Interfacial tension determines many characteristics of biological condensates (19, 50, 52, 54–59). For example, liquid-like condensates adopt a spherical shape in order to minimize the surface area under the influence of interfacial tension

(52, 54, 58), and they exhibit a wetting phenomenon when in contact with other immiscible phases with appropriate surface properties, so as to minimize the whole free energy of the system (57, 59). Furthermore, interfacial tension drives coalescence of two encountering liquid-like condensates: a higher interfacial tension increases the fusion propensity and accelerates the fusion process (19, 50, 54–56, 58, 60). Other effects such as Ostwald ripening, a process in which larger condensates grow by absorbing components from smaller condensates, is also driven by interfacial tension (61, 62). Following LLPS induction *in vitro* and *in vivo*, the growth/coarsening of biological condensates is governed by Ostwald ripening and coalescence. These two processes determine the size and distribution of biological condensates in living cells, although Ostwald ripening is often limited *in vivo via* various mechanisms such as posttranslational modifications of proteins (63–66). Biological condensates also restrict their size by adsorbing nanometer-scale protein clusters onto their surface, which decrease their interfacial tension and prevent the droplets coarsening (67).

The interfacial tension also controls the interaction between immiscible biological condensates (Fig. 2*D*). Examples include the assembly of "phase in phase" condensates, such as the nucleolus for stepwise rRNA production and processing (57, 68), packaging of membrane-bound liquid condensates such as autophagosomes in protein aggrephagy (32, 59, 69), organization of liquid condensate-coated membrane organelles/structures such as synaptic vesicle reservoirs in presynaptic terminal boutons of synapses (70, 71), and association between multiple phases such as attachment of granules formed by the RNA-binding protein TIS11B (TIS granules) onto the ER which enables 3′UTR-mediated protein–protein interaction and formation of PZM (P granules, Z granules, and *Mutator* foci) granules in *C. elegans* germline development (72, 73). Notably, bio-membranes are also phase-separated biological condensates, which adopt a liquid-crystal arrangement. Bio-membranes frequently interact with other biological condensates, for example, to build up membrane contact sites and associate with protein condensates (74, 75). The primary principle for these multi-phase interactions is to decrease the total free energy of the system (52, 57, 59, 67). Therefore, a change of interfacial tension can determine the final architecture of the multi-phase organization.

The physical properties of the dilute phase and/or external environment affect the dynamics and function of biological condensates

The dense phase and dilute phase of an equilibrated phase-separation system are in thermodynamic equilibrium in a fixed environment. Thus, any changes in the dilute phase and/or the external environment disrupt this balance and result in altered phase separation and/or material properties of the biological condensates and consequently their physiological functions. For example, mTORC1 regulates the viscosity of the cytoplasm *via* tuning the ribosome concentration to modulate the formation of cytosolic biological condensates (76), various nuclear protein condensates tend to form and grow in regions with low stiffness and density (52), and mechanical shear forces from the external environment induce liquid-to-solid transition of various protein condensates (77). The cell harnesses these mechanisms to modulate the functions of biological condensates under various conditions. For example, the poly(A)-binding protein Pab1 undergoes phase separation and transition at elevated temperatures to form gel-like structures, which is important for yeast to survive under heat stress conditions (78). In addition, Sup35 undergoes phase separation in response to a reduction in cytosolic pH to promote yeast cellular fitness (79). Similarly, the thermosensitivity of *Arabidopsis* is specified by the length of a prion-like domain in ELF3, which undergoes LLPS in response to elevated temperature (80); while fiber formation in spider silk relies on a series of environmental influences, including evaporation of water, elongational flow, and shear forces (81, 82). Thus, the physiological functions of biological condensates can be modulated by the physical properties and dynamic variation of the dilute phase and/or the external environment.

The different physicochemical environments in the dilute phase and the dense phase can also have distinct effects on biological pathways. For example, ER-associated TIS granules enable specific protein–protein interactions which are not detected outside the granules (72). A possible explanation for such specific interactions is that biological condensates are capable of concentrating certain factors while excluding others (3, 13, 34, 83). Within biological condensates, the characteristic viscosity affects the diffusivity of the components, which changes their interaction and/or reaction efficiency in certain biological processes (83). The different physicochemical environments inside biological condensates, such as crowding and polarity, may also induce allosteric effects in the components, thus affecting the thermodynamic favorability of the interactions and/or reactions (84). At present, we do not have methods for systematically characterizing the physiochemical environments of biological condensates and the dilute phase *in vivo*, or the biological consequences when these environments change. However, as described in the next sections, we are beginning to make progress in defining the material properties of biologically relevant condensates.

Classic methods for characterizing the material properties of biological condensates

A number of techniques have been developed to study the material properties of biological condensates in *in vitro* systems, and a few of them can also be applied to condensates formed in living cells. Several methods have been adopted to characterize phase separation in *in vitro* systems using recombinantly purified proteins or synthetic DNAs/RNAs (reviewed in Ref. 85). If a system undergoes phase separation and yields liquid droplets, it becomes turbid, and the turbidity can be measured using a spectrophotometer. The morphological structure of liquid droplets generated *in vitro* can be observed on a microscope using bright-field imaging, differential interference contrast imaging, or fluorescence imaging. Fluorescence labeling of biomacromolecules can cause artificial effects in LLPS systems, and therefore results obtained using this approach should be cautiously verified by other

examinations, which will be discussed below. Liquid droplets are spherical due to interfacial tension when suspended in a solution. Biomacromolecules undergoing phase separation in *in vivo* systems (*e.g.*, cell lines) are generally labeled with fluorescent tags or stained by specific antibodies and can be observed to form punctate structures *via* fluorescence imaging. Total internal reflection fluorescence microscopy, structured illumination microscopy, stochastic optical reconstruction microscopy, and other super-resolution imaging techniques are used to optimize both the temporal and spatial resolution. The total extent of phase separation of certain components can be roughly estimated from sedimentation assays, in which phase-separated condensates are separated from the surrounding medium by ultracentrifugation (85). Below, we describe several methods for further characterizing the material properties of biological condensates.

FRAP assay

As mentioned earlier in this review, the FRAP assay is generally used to characterize the liquidity of biological condensates. This assay is performed with fluorescently labeled biomolecules. For proteins, a genetically encoded fluorescent tag can be recombinantly added to the N- or C-terminus, or a fluorescent probe can be conjugated onto the primary amines, carboxylic acid moieties, or free thiols. Fluorescence labeling, to some degree, affects the conformation and chemical properties of biomacromolecules and subsequently influences the material properties of assembled biological condensates. This should be remembered when the results are considered. Dilution of fluorescently labeled biomacromolecules with unlabeled ones in appropriate proportions can reduce the undesired effects. The influences of labeled fluorescent tags or probes can be evaluated by using sedimentation assays to examine and compare the extent to which labeled and unlabeled proteins phase separate. Similarly, the phenotypes of fusion, wetting, and deformation, which are detected *via* bright-field or differential interference contrast microscopy, can also be employed to judge the influences of fluorescence labeling on the material properties of biological condensates.

The FRAP assay can be performed on a confocal microscope. Regions of interest are selected for bleaching with an appropriate laser, and the fluorescence intensities of these regions are recorded with time and plotted as a fluorescence recovery curve. Biological condensates with liquid properties have a much faster recovery rate, while the recovery rate for gel- and solid-like condensates is very slow or hard to detect (Fig. 3*A*). The diffusivity of certain components can be calculated from the fluorescence recovery curve, and the viscosity of the condensates can be roughly estimated from the diffusivity *via* the Stokes-Einstein equation (50, 54). The calculated diffusivity, however, may be different when different models are used to fit the curve (86). Also, as mentioned above, the fluidity of different components or of the same component in different regions of the condensates can vary. FRAP analyses of multiple components and also of distinct regions of interest are needed, and the results should be cautiously interpreted. Selecting different portions of the condensates for bleaching, for example, the whole droplet, half of the droplet, or a small portion of the droplet, can also generate different diffusivity values (86). This may arise from the distinct concentrations and diffusivities of fluorescent components inside and outside of the droplets and also the interfacial resistance to mass transfer (86). Nevertheless, as a simple and convenient assay, and as one of the few assays that can be used for characterizing biological condensates *in vivo*, the FRAP assay is still widely used in the field of biological phase separation/transition.

Fusion assay

The fusion assay can be used to characterize the liquidity, interfacial tension, and viscosity of biological condensates. Liquid condensates often undergo fusion to form larger ones upon encounter both *in vitro* and *in vivo* and then shrink into a spherical shape due to their flowable interior and interfacial tension. Gel- and solid-like condensates seldom undergo fusion events, since they do not deform easily upon encounter. Two *in vitro* assembled condensates can be labeled with different fluorescent probes for fusion analysis, and the diffusion of the internal molecules inside the coalescing droplets can be detected with time (51). The rate for two coalescing liquid condensates to recover into a spherical one is largely determined by the ratio of interfacial tension to viscosity (γ/η). The former drives coalescence, while the latter resists it. Therefore, the ratio of γ/η can be roughly estimated by plotting the fusion relaxation time against the length scale of the two coalescing liquid condensates (Fig. 3*B*) (50, 54–57, 67).

Fission of liquid condensates can sometimes be detected and also reflects the liquidity of biological condensates (32). However, fission of liquid condensates occurs much less frequently than fusion. Fission is more dependent on external forces than fusion and may occur more frequently *in vivo* than *in vitro* because living cells can provide the necessary energy.

Chemical/salt resistance assays

These kinds of assays are used to roughly determine the liquidity or the degree of transition (liquid-to-gel or liquid-to-solid) of phase-separated droplets. The intermolecular interactions within phase-separated droplets, which maintain them as distinct phases in solution, are sensitive to changes in the surrounding environment. Condensates with liquid properties are generally more sensitive to environmental changes, as the intermolecular interactions inside liquid condensates are usually weak. Addition of salts (*e.g.*, NaCl) or organic reagents (*e.g.*, 1,6-hexanediol) that increase the ionic strength or hydrophobicity of the solution may result in dissolution of the liquid droplets (32, 87, 88), while gel-like and solid-like condensates exhibit different degrees of resistance to disassembly upon environmental change (Fig. 3*C*). Gel-like condensates, in some cases, can also be dissolved by organic reagents, such as 1,6-hexanediol (89). Thus, this assay is generally employed as an auxiliary approach to characterize the material states of phase-separated droplets. The chemical/salt resistance assay can be combined with sedimentation analysis to determine the influence of environmental change on the extent of phase separation.

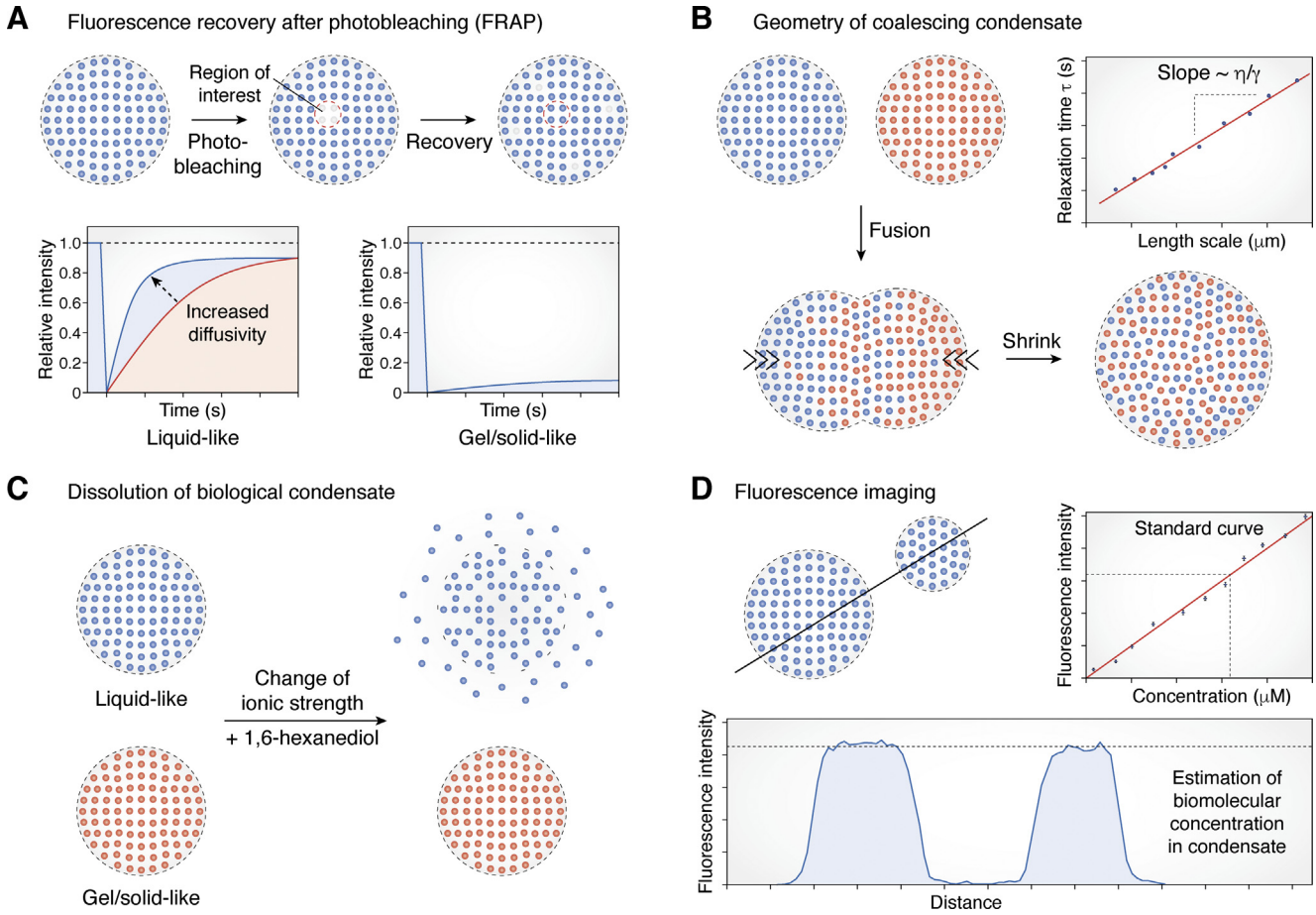

Figure 3. Methods for characterizing the material properties of biological condensates. *A*, schematic showing the principle of the fluorescence recovery after photobleaching (FRAP) assay. A region of interest (ROI) (*red dotted circle*) is chosen for photobleaching, and the fluorescence intensity of the ROI is measured with time. The intensity recovers quickly for biological condensates with high fluidity but recovers slowly for gel/solid-like condensates. *B*, biological condensates with liquid properties undergo fusion upon encounter. Driven by the interfacial tension, the fusing condensates shrink to a spherical shape over time. The speed for a coalescing condensate to reshape can be used to roughly estimate the ratio of interfacial tension against viscosity (γ/η). *C*, in general cases, biological condensates with liquid-like but not gel/solid-like properties may be dissolved by changing the ionic strength or adding 1,6-hexanediol. In some cases, gel-like condensates may also be dissolved by 1,6-hexanediol. *D*, schematic showing the estimation of biomolecular concentration inside biological condensates based on fluorescence imaging. The fluorescence intensity of a certain component in phase-separated condensates is measured on a confocal microscope, and the concentration is back-calculated from a standard curve of fluorescence intensity against molecular concentration.

Concentration estimation based on fluorescence imaging

The concentration of components in the dense phase and dilute phase in *in vitro* recombinant LLPS systems can be estimated by determining the fluorescence intensity on a confocal microscope (13, 90). First, a standard curve is plotted to show the fluorescence intensity of the measured component at various concentrations. Then, the fluorescence intensity of the component in phase-separated condensates is measured and the concentration is back-calculated from the standard curve (Fig. 3*D*). The fluorescence intensity in the dilute phase is usually too weak to be precisely measured but can be calculated based on the extent of phase separation of the component, as estimated from sedimentation assays. This method can also be used to measure the concentration of certain components in biological condensates *in vivo* but with less precision (91, 92).

The concentration of a component in biological condensates can also be estimated by NMR spectroscopy using a similar principle as the imaging method. Firstly, the ^{1}H signal intensity of a dilute sample of the component is acquired from the NMR spectrum. Then, the concentration in the LLPS condensed phase is calculated by comparing the ^{1}H signal intensity of the condensate to that of the dilute sample (93). Currently, however, this NMR spectrum-based method can only be performed on *in vitro*-prepared LLPS systems.

Newly emerging techniques for measuring the material properties of biological condensates

Many physical and analytical chemistry techniques are used to measure the material properties of liquid phases with sizes on the centimeter or millimeter scale. The size of biological condensates, however, is generally on the micrometer or nanometer scale. In this part, we will introduce several modified physicochemical techniques for studying the material properties of biological condensates.

Atomic force microscopy

The atomic force microscopy (AFM) technique has been widely used in studying the surface morphology, heterogeneity, viscoelasticity, surface/interfacial tension, and interaction forces of materials. All AFM analyses are based on measuring the interaction forces between the scanning probe and the specimen (Fig. 4*A*, left). In brief, the studied specimen is placed on a stage which is precisely controlled to rise and fall by a piezoceramics, thus bringing the specimen into contact with the probe, or separating the specimen from the probe. The scanning probe is fixed on a cantilever with a known spring coefficient. Based on the degree of bending of the cantilever, the interaction forces on the probe can be calculated. The bending of the cantilever is detected by a laser beam, which is reflected by the cantilever and illuminates a photodiode. Different shapes can be used for the tip of the AFM scanning probe. A conical probe is most often used for surface morphological scanning of materials, but other types, such as spherical and cylindrical probes, are also adopted to study biological condensates.

Several recent studies employed AFM to detect the formation, morphology, and heterogeneity of biological condensates

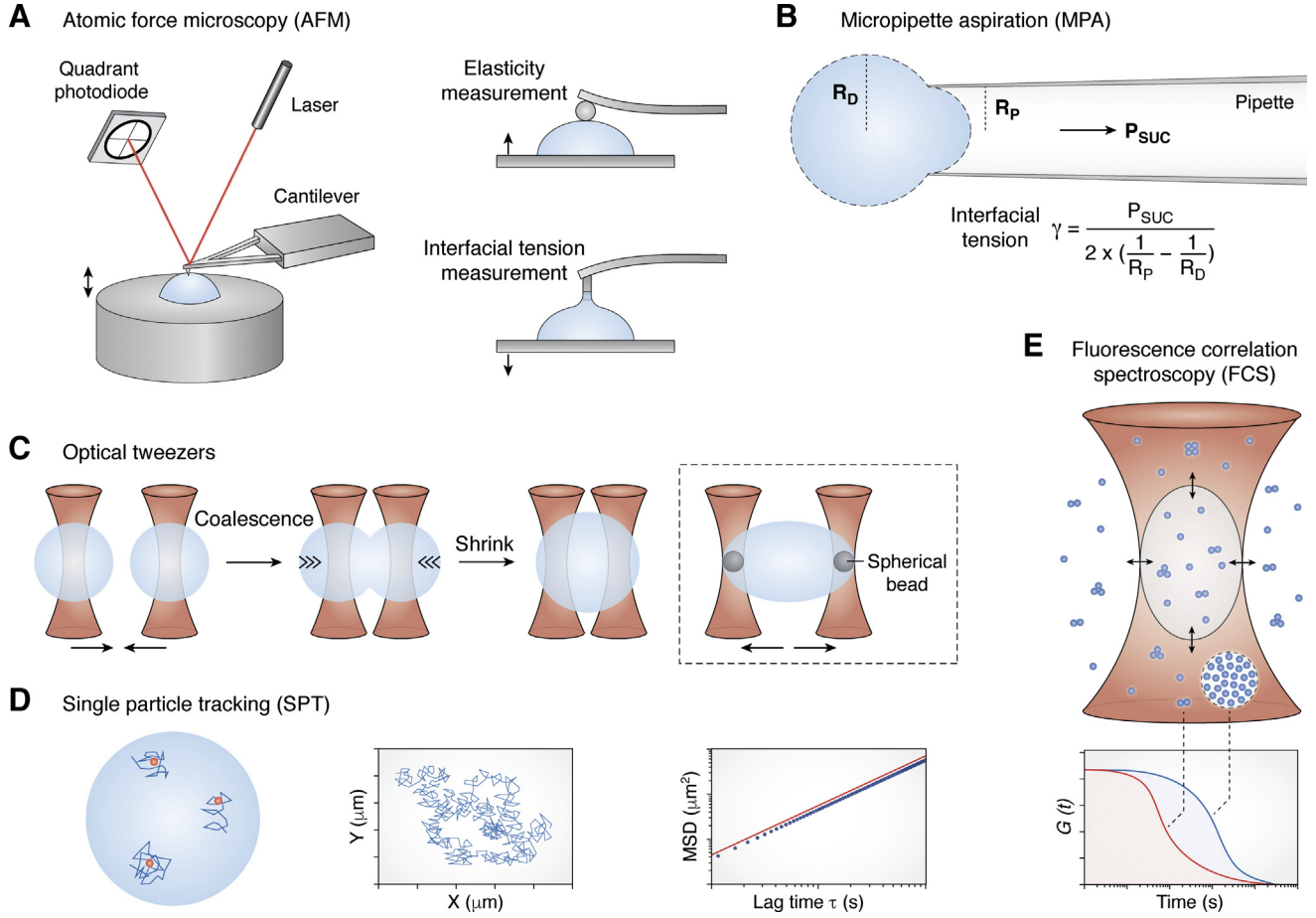

Figure 4. Techniques for measuring the material properties of biological condensates. *A*, schematic showing the working principle of atomic force microscopy (AFM). The specimen, fixed on a piezoceramic stage, is contacted by a scanning probe attached on a cantilever with known spring coefficient. The interaction force can be calculated from bending of the cantilever, which is detected by a reflected laser beam (*A*, *left*). Various types of probe tip can be chosen for different applications. A spherical probe tip is generally used to measure the elasticity of biological condensates, while a cylindrical probe tip is generally used to estimate the interfacial tension (*A*, *right*). *B*, schematic showing the measurement of interfacial tension of biological condensates by the micropipette aspiration (MPA) technique. A droplet is captured by the micropipette and deformed by a negative suction pressure (P_{SUC}) to form a hemisphere within the micropipette. When a stable state is reached, the interfacial tension γ is calculated from the radii of both the droplet (R_D) and the micropipette (R_P) by the equation presented below the schematic. *C*, the optical tweezers technique provides a noncontact method for manipulating *in vitro* assembled biological condensates. Two biological droplets, held *via* dual-trap optical tweezers, can be moved together so that they coalesce. This allows measurement of the interfacial tension during the fusion process (*C*, *left*). Two spherical beads packaged into a single droplet can be manipulated to stretch the droplet by a dual-trap optical tweezers system at fixed frequencies. This allows estimation of the viscoelastic properties and the interfacial tension of biological condensates (*C*, *right*). *D*, schematic presenting the measurement of viscosity inside biological condensates by the single-particle tracking (SPT) technique. Single-particle probes are packaged into the biological condensates, and the trajectories are tracked by video imaging. The mean square displacement (MSD) of individual particles is calculated from the trajectories and plotted against lag time (τ) and further used to estimate the diffusivity coefficient (*D*) of the particles. The viscosity η is then calculated from *D* with the Stokes-Einstein equation. *E*, schematic showing the principle of the fluorescence correlation spectroscopy (FCS) technique in studying biological condensates. An excitation volume (*gray oval*) is created by the FCS microscope and the fluctuation of fluorescence intensity of labeled biomacromolecules inside the detected volume due to Brownian diffusion is recorded for a certain time. The acquired data are used to generate a correlation curve, from which the material properties of the studied biomolecules, such as the concentration, diffusivity and hydraulic radius, can be calculated. Biomacromolecular particles with different diffusivity and hydraulic radius, such as oligomers and condensates of the same biomacromolecule, generate distinct correlation curves.

under various conditions in *in vitro* LLPS systems (69, 94–96). Using high-speed AFM, the dynamic surface motion of biological condensates can also be measured (69). The scanning probes used in these studies were conical, in order to minimize the contact area between probe and specimen. However, a spherical probe is generally used for precise measurement of the elasticity of biological condensates, for which purpose the contact area must be known (Fig. 4*A*, top right). A recent study explored the use of AFM equipped with a spherical probe to estimate the elasticity of *in vitro* assembled PSD condensates (13). In addition, the AFM technique is capable of measuring the interfacial tension of liquid materials using a cylindrical probe, although this has yet to be attempted for biological condensates (Fig. 4*A*, bottom right) (97).

Micropipette aspiration assay

The interfacial tension of *in vitro* assembled liquid biological condensates can also be measured by the micropipette aspiration technique (97, 98). The micropipette aspiration assay is performed on a bright-field microscope with a micromanipulation device. A micropipette with the inner diameter on the micrometer scale is fixed on the micromanipulation device and operated to capture a biological condensate in the *in vitro* LLPS system. A suitable negative pressure is applied to the surface of the captured biological droplet through the micropipette, so as to just generate a deformation on the surface of the biological droplet (Fig. 4*B*). Complete suction of the droplet into the micropipette should be avoided. To measure the interfacial tension of the condensates, the sucked portion inside the micropipette should be a hemisphere. When the deformation stops and the sucked droplet reaches a stable state, the radii of both the droplet and the micropipette (R_D and R_P, respectively) and also the negative pressure (P_{SUC}) are recorded. The interfacial tension of the biological condensate is calculated from the equation $\gamma = \frac{P_{SUC}}{2\times\left(\frac{1}{R_P}-\frac{1}{R_D}\right)}$. This technique has been used to measure the interfacial tension of purified lipid droplets, which are phase-separated condensates of bio-lipids (98).

Optical tweezers

Estimation of the interfacial tension of biological condensates *via* fusion assays, which is described above, has several technical and practical limitations. Firstly, since suspended biological condensates are not still but moving in the LLPS system, fusion events can only be recorded for condensates which sink onto the surface of the glass slide. Thus, the interactions between the condensates and the glass surface may interfere with the coalescence process. Secondly, the duration of the fusion process for some biological condensates is too short to be recorded by video imaging. Thirdly, in some cases, fusion events are very rare, which greatly increases the investigator workload. To overcome these limitations, several recent studies analyzed fusion processes by using optical tweezers to manipulate two suspended biological condensates (Fig. 4*C*, left) (20, 99–102). In the dual-trap optical tweezers system, two droplets are trapped by two different focused laser beams. One laser beam and its trapped droplet are fixed, while the other one moves and brings its trapped droplet into contact with the fixed droplet for coalescence. The fusion processes are then recorded for further analysis. Moreover, the laser signal or force from the moved optical trap can be recorded and used to accurately extract the relaxation time for fusion events (20, 101).

The dual-trap optical tweezers technique has also been used to study the rheology and interfacial tension of protein condensates (Fig. 4*C*, right) (103). In this assay, spherical beads are added into the LLPS system and packaged into newly formed protein condensates. Two optical traps are then used to trap two beads located at the opposite sides of a single protein condensate. One optical trap is fixed and the other one moves away from the fixed trap until the droplet is slightly stretched. The moving trap is then set to oscillate at several predefined frequencies. The force from the optical traps is recorded for further analysis, and calculation of the frequency-dependent viscoelastic properties and also the interfacial tension of the protein condensates.

Single-particle tracking assay

As a classic microrheology technique, single-particle tracking (SPT) is widely used in measuring the viscoelastic properties of liquid materials. SPT has been explored for estimating the viscosity of *in vitro* assembled biological condensates such as LAF-1 droplets and Whi3 droplets (Fig. 4*D*) (55–57, 67, 104, 105). Spherical nanoparticles or microparticles are packaged into biological condensates, and the Brownian motion of individual particles over a certain duration is recorded by video imaging on a bright-field microscope for nonfluorescent particles or a fluorescence microscope for fluorescent particles. To avoid nonspecific adsorption, the spherical particles are often first passivated with inert polymers such as PEG. The trajectories of individual particles with time are mapped. From the trajectory data, the location of individual particles as a function of time and the consequent mean square displacement are calculated and plotted against the lag time τ. Multiple particles can be monitored at the same time. The diffusion coefficient (D) of individual particles over the analysis period can then be estimated from the equation $MSD(\tau) = 4D\tau^{\alpha}$, where α represents the confinement state of the diffusing particle, which equals 1 for classical Brownian motion in a viscous liquid. The viscosity is further calculated from D by the Stokes-Einstein equation.

A modified SPT technique using optically anisotropic gold nanorod (AuNR) probes has recently been developed to monitor the spatial subcompartments and temporal changes of viscosity inside *in vitro* assembled p62 condensates (105). AuNR probes (90 × 40 nm for unmodified and 105 × 50 nm for modified AuNRs) packaged into p62 condensates are tracked by a high-speed camera (∼50 frames per second) in a dark-field microscope. This modified SPT technique allows spatial and temporal analysis of the translational diffusional dynamics of the AuNRs. Several subregions with slightly different viscosities coexist inside a

single p62 condensate, and the viscosity significantly changes with time, which reflects the liquid-to-solid transition of p62 condensates (105).

Fluorescence correlation spectroscopy

The fluorescence correlation spectroscopy (FCS) technique has recently been utilized to estimate the concentration and diffusivity of biomolecules both inside and outside of biological condensates (104, 106–109). The FCS technique measures the fluctuation of fluorescence intensity, which occurs due to Brownian diffusion and/or physicochemical reactions of fluorescent molecules. FCS analyses a micro-excitation volume as small as 10^{-15} L, so as to back-calculate the hydraulic properties and behaviors of a single molecule (Fig. 4*E*). The FCS assay is performed on a fluorescence correlation microscope, and the fluctuation of fluorescence intensity in the excitation volume is recorded for a fixed time interval. A correlation curve against time is generated from the recorded data, from which the concentration, diffusivity, and hydraulic radius of the studied fluorescent biomolecule can be calculated. The excitation area can be set completely inside or outside of the studied biological condensates to estimate the material properties of the dense phase or the dilute phase, respectively. A recent study also used a newly developed dual-color fluorescence cross-correlation spectroscopy method to capture the formation of nanoscale condensates, so as to estimate the critical concentration for phase separation at the nanoscale (107). The size and growth rate of biological condensates and the molecular composition and binding affinity of the internal biomolecules were measured. The FCS technique can also be easily performed in living cells (108, 109), which may yield exciting future discoveries in the field of biological condensates.

Microfluidic devices

Microfluidic devices contain millimeter-sized chambers or micrometer-sized channels to confine and manipulate the fluid flow and study the behavior of the fluid or objects (such as cells or droplets) flowing with the liquid (110, 111). Depending on the purpose of the study, different chamber or channel designs can be employed. Considering their underlying principles, microfluidic technologies have several advantages for studying biological condensates (112) and may evolve to be a powerful technique in quantifying the material properties of condensates.

A microfluidic platform has been introduced to study the liquidity behaviors of biological condensates (113). With this platform, the coalescence of condensates can be studied by flowing the condensates into the device where the inlet is filled with polydimethylsiloxane pillars. Condensates collide and coalesce with the assistance of the pillars and the coalescence events can be monitored under a microscope. Tracer beads can also be used in this platform: the motion of the tracer beads inside the coalesced condensates can be tracked and the viscosity of the condensates can be estimated by the above-mentioned single-particle tracking measurements. Moreover, different solutions can be injected from different channels then mixed inside the device. This allows the observation of more complex phenomena and analysis of various properties of the condensates.

A microfluidic phase chip has been developed to measure the saturation concentration of condensates over several orders of magnitude under various solution conditions (114). Compared with manual experiments, the chip allows measurements with a much smaller sample yet offers better statistics.

Conclusions and outlook

Multiple physicochemical methods are now available for the study of phase separation and transition. These techniques provide powerful tools for exploring the role of the material properties of biological condensates in their physiological functions. It should be noted that for the same biological condensate, the values of material properties estimated by different methods may vary. This is possibly due to objective differences arising from the principles and system errors of the various methods and also to the technical and practical limitations of each approach. Therefore, it is rational to compare the material properties measured by the same method on different biological condensates or condensates formed under different conditions. In the near future, there is an urgent requirement to develop more techniques suitable for high-accuracy *in vivo* studies. Additional techniques that have been used in the field of physics and chemistry and also other aspects of biology, such as structural biology and single-molecule biophysics, could be adapted for characterizing phase-separated biological condensates. For example, Raman imaging, which is employed to analyze the internal structures and physicochemical properties of materials, can potentially be developed to characterize and measure the material properties of biological condensates both *in vitro* and *in vivo*. Single molecular mechanics techniques, such as biomembrane force probe spectroscopy, can also be modified for further exploration of the mechanical properties of biological condensates (8). The cryo-EM and 3D tomography techniques may possibly be used for resolving the arrangement, organization, and even the atomic structure of the internal constituents of biological condensates. The introduction of more techniques will greatly advance our understanding of how the material properties of biological condensates modulate their physiological functions. These advances will also help us understand the detrimental effects resulting from abnormal phase separation and/or transition under pathological conditions. Modulating the material states of pathological condensates has become a promising therapeutic strategy in various diseases associated with abnormal phase separation and transition of biological condensates.

Acknowledgments—We are grateful to Dr Isabel Hanson for editing work.

Author contributions—Z. W. and H. Z. conceptualization; Z. W., J. L., and H. Z. writing–original draft; J. L. and H. Z. writing–review and editing.

Funding and additional information—This work was supported by the following grants: National Natural Science Foundation of China (82188101, 92054301, and 31790403 to H. Z. and 31871426 to Z. W.) and Chinese Ministry of Science and Technology (2017YFA0503401 to H. Z.).

Conflict of interest—The authors declare that they have no conflicts of interest with the contents of this article..

Abbreviations—The abbreviations used are: AFM, atomic force microscopy; AuNR, optically anisotropic gold nanorod; ER, endoplasmic reticulum; FCS, fluorescence correlation spectroscopy; FRAP, fluorescence recovery after photobleaching; IDRs, intrinsically disordered regions; LCRs, low complexity regions; PSD, postsynaptic density; RNP, ribonucleoprotein; SGs, stress granules; SPT, Single-particle tracking.

References

1. Boeynaems, S., Alberti, S., Fawzi, N. L., Mittag, T., Polymenidou, M., Rousseau, F., Schymkowitz, J., Shorter, J., Wolozin, B., Van Den Bosch, L., Tompa, P., and Fuxreiter, M. (2018) Protein phase separation: A new phase in cell biology. *Trends Cell Biol.* **28**, 420–435
2. Shin, Y., and Brangwynne, C. P. (2017) Liquid phase condensation in cell physiology and disease. *Science* **357**, eaaf4382
3. Banani, S. F., Lee, H. O., Hyman, A. A., and Rosen, M. K. (2017) Biomolecular condensates: Organizers of cellular biochemistry. *Nat. Rev. Mol. Cell Biol.* **18**, 285–298
4. Woodruff, J. B., Wueseke, O., Viscardi, V., Mahamid, J., Ochoa, S. D., Bunkenborg, J., Widlund, P. O., Pozniakovsky, A., Zanin, E., Bahmanyar, S., Zinke, A., Hong, S. H., Decker, M., Baumeister, W., Andersen, J. S., *et al.* (2015) Centrosomes. Regulated assembly of a supramolecular centrosome scaffold *in vitro*. *Science* **348**, 808–812
5. Berchowitz, L. E., Kabachinski, G., Walker, M. R., Carlile, T. M., Gilbert, W. V., Schwartz, T. U., and Amon, A. (2015) Regulated formation of an amyloid-like translational repressor governs gametogenesis. *Cell* **163**, 406–418
6. Kaganovich, D. (2017) There is an inclusion for that: Material properties of protein granules provide a platform for building diverse cellular functions. *Trends Biochem. Sci.* **42**, 765–776
7. Wang, Z., and Zhang, H. (2019) Phase separation, transition, and autophagic degradation of proteins in development and pathogenesis. *Trends Cell Biol.* **29**, 417–427
8. Zhang, H., Ji, X., Li, P., Liu, C., Lou, J., Wang, Z., Wen, W., Xiao, Y., Zhang, M., and Zhu, X. (2020) Liquid-liquid phase separation in biology: Mechanisms, physiological functions and human diseases. *Sci. China Life Sci.* **63**, 953–985
9. Alberti, S., and Hyman, A. A. (2016) Are aberrant phase transitions a driver of cellular aging? *Bioessays* **38**, 959–968
10. Israelachvili, J. N. (2011) *Intermolecular and Surface Forces*, 3rd Edition, Academic Press, Cambridge
11. Li, P. L., Banjade, S., Cheng, H. C., Kim, S., Chen, B., Guo, L., Llaguno, M., Hollingsworth, J. V., King, D. S., Banani, S. F., Russo, P. S., Jiang, Q. X., Nixon, B. T., and Rosen, M. K. (2012) Phase transitions in the assembly of multivalent signalling proteins. *Nature* **483**, 336–340
12. Zeng, M., Shang, Y., Araki, Y., Guo, T., Huganir, R. L., and Zhang, M. (2016) Phase transition in postsynaptic densities underlies formation of synaptic complexes and synaptic plasticity. *Cell* **166**, 1163–1175.e12
13. Zeng, M., Chen, X., Guan, D., Xu, J., Wu, H., Tong, P., and Zhang, M. (2018) Reconstituted postsynaptic density as a molecular platform for understanding synapse formation and plasticity. *Cell* **174**, 1172–1187.e16
14. Jain, A., and Vale, R. D. (2017) RNA phase transitions in repeat expansion disorders. *Nature* **546**, 243–247
15. Yang, P. G., Mathieu, C., Kolaitis, R. M., Zhang, P. P., Messing, J., Yurtsever, U., Yang, Z. M., Wu, J. J., Li, Y. X., Pan, Q. F., Yu, J. Y., Martin, E. W., Mittag, T., Kim, H. J., and Taylor, J. P. (2020) G3BP1 is a tunable switch that triggers phase separation to assemble stress granules. *Cell* **181**, 325–345.e28
16. Guillen-Boixet, J., Kopach, A., Holehouse, A. S., Wittmann, S., Jahnel, M., Schlussler, R., Kim, K., Trussina, I. R. E. A., Wang, J., Mateju, D., Poser, I., Maharana, S., Ruer-Gruss, M., Richter, D., Zhang, X. J., *et al.* (2020) RNA-induced conformational switching and clustering of G3BP drive stress granule assembly by condensation. *Cell* **181**, 346–361.e17
17. Sanders, D. W., Kedersha, N., Lee, D. S. W., Strom, A. R., Drake, V., Riback, J. A., Bracha, D., Eeftens, J. M., Iwanicki, A., Wang, A., Wei, M. T., Whitney, G., Lyons, S. M., Anderson, P., Jacobs, W. M., *et al.* (2020) Competing protein-RNA interaction networks control multiphase intracellular organization. *Cell* **181**, 306–324.e28
18. Yamazaki, T., Souquere, S., Chujo, T., Kobelke, S., Chong, Y. S., Fox, A. H., Bond, C. S., Nakagawa, S., Pierron, G., and Hirose, T. (2018) Functional domains of NEAT1 architectural lncRNA induce paraspeckle assembly through phase separation. *Mol. Cell* **70**, 1038–1053.e7
19. Saha, S., Weber, C. A., Nousch, M., Adame-Arana, O., Hoege, C., Hein, M. Y., Osborne-Nishimura, E., Mahamid, J., Jahnel, M., Jawerth, L., Pozniakovski, A., Eckmann, C. R., Julicher, F., and Hyman, A. A. (2016) Polar positioning of phase-separated liquid compartments in cells regulated by an mRNA competition mechanism. *Cell* **166**, 1572–1584.e16
20. Patel, A., Lee, H. O., Jawerth, L., Maharana, S., Jahnel, M., Hein, M. Y., Stoynov, S., Mahamid, J., Saha, S., Franzmann, T. M., Pozniakovski, A., Poser, I., Maghelli, N., Royer, L. A., Weigert, M., *et al.* (2015) A liquid-to-solid phase transition of the ALS protein FUS accelerated by disease mutation. *Cell* **162**, 1066–1077
21. Molliex, A., Temirov, J., Lee, J., Coughlin, M., Kanagaraj, A. P., Kim, H. J., Mittag, T., and Taylor, J. P. (2015) Phase separation by low complexity domains promotes stress granule assembly and drives pathological fibrillization. *Cell* **163**, 123–133
22. Alberti, S. (2017) The wisdom of crowds: Regulating cell function through condensed states of living matter. *J. Cell Sci.* **130**, 2789–2796
23. Klosin, A., Oltsch, F., Harmon, T., Honigmann, A., Julicher, F., Hyman, A. A., and Zechner, C. (2020) Phase separation provides a mechanism to reduce noise in cells. *Science* **367**, 464–468
24. Riback, J. A., and Brangwynne, C. P. (2020) Can phase separation buffer cellular noise? *Science* **367**, 364–365
25. Stoeger, T., Battich, N., and Pelkmans, L. (2016) Passive noise filtering by cellular compartmentalization. *Cell* **164**, 1151–1161
26. Holehouse, A. S., and Pappu, R. V. (2018) Functional implications of intracellular phase transitions. *Biochemistry* **57**, 2415–2423
27. Riback, J. A., Zhu, L., Ferrolino, M. C., Tolbert, M., Mitrea, D. M., Sanders, D. W., Wei, M. T., Kriwacki, R. W., and Brangwynne, C. P. (2020) Composition-dependent thermodynamics of intracellular phase separation. *Nature* **581**, 209–214
28. Saunders, T. E., Pan, K. Z., Angel, A., Guan, Y., Shah, J. V., Howard, M., and Chang, F. (2012) Noise reduction in the intracellular pom1p gradient by a dynamic clustering mechanism. *Dev. Cell* **22**, 558–572
29. Eldar, A., and Elowitz, M. B. (2010) Functional roles for noise in genetic circuits. *Nature* **467**, 167–173
30. Strome, S. (2005) *Specification of the Germ Line*. WormBook: 1–10
31. Zhang, Y., Yan, L., Zhou, Z., Yang, P., Tian, E., Zhang, K., Zhao, Y., Li, Z., Song, B., Han, J., Miao, L., and Zhang, H. (2009) SEPA-1 mediates the specific recognition and degradation of P granule components by autophagy in C. elegans. *Cell* **136**, 308–321
32. Zhang, G., Wang, Z., Du, Z., and Zhang, H. (2018) mTOR regulates phase separation of PGL granules to modulate their autophagic degradation. *Cell* **174**, 1492–1506.e22
33. Boke, E., Ruer, M., Wuhr, M., Coughlin, M., Lemaitre, R., Gygi, S. P., Alberti, S., Drechsel, D., Hyman, A. A., and Mitchison, T. J. (2016) Amyloid-like self-assembly of a cellular compartment. *Cell* **166**, 637–650
34. Su, X., Ditlev, J. A., Hui, E., Xing, W., Banjade, S., Okrut, J., King, D. S., Taunton, J., Rosen, M. K., and Vale, R. D. (2016) Phase separation of signaling molecules promotes T cell receptor signal transduction. *Science* **352**, 595–599

35. Nong, J. X., Kang, K. X., Shi, Q. N., Zhu, X. C., Tao, Q. H., and Chen, Y. G. (2021) Phase separation of Axin organizes the beta-catenin destruction complex. *J. Cell Biol.* **220**, e202012112
36. Du, M. J., and Chen, Z. J. J. (2018) DNA-induced liquid phase condensation of cGAS activates innate immune signaling. *Science* **361**, 704–709
37. Nedelsky, N. B., and Taylor, J. P. (2019) Bridging biophysics and neurology: Aberrant phase transitions in neurodegenerative disease. *Nat. Rev. Neurol.* **15**, 272–286
38. Mathieu, C., Pappu, R. V., and Taylor, J. P. (2020) Beyond aggregation: Pathological phase transitions in neurodegenerative disease. *Science* **370**, 56–60
39. Nil, Z., Hervás, R., Gerbich, T., Leal, P., Yu, Z. L., Saraf, A., Sardiu, M., Lange, J. J., Yi, K. X., Unruh, J., Slaughter, B., and Si, K. (2019) Amyloid-like assembly activates a phosphatase in the developing drosophila embryo. *Cell* **178**, 1403–1420.e21
40. Weidtkamp-Peters, S., Lenser, T., Negorev, D., Gerstner, N., Hofmann, T. G., Schwanitz, G., Hoischen, C., Maul, G., Dittrich, P., and Hemmerich, P. (2008) Dynamics of component exchange at PML nuclear bodies. *J. Cell Sci.* **121**, 2731–2743
41. Chalupnikova, K., Lattmann, S., Selak, N., Iwamoto, F., Fujiki, Y., and Nagamine, Y. (2008) Recruitment of the RNA helicase RHAU to stress granules *via* a unique RNA-binding domain. *J. Biol. Chem.* **283**, 35186–35198
42. Sun, D. X., Wu, R. B., Zheng, J. X., Li, P. L., and Yu, L. (2018) Polyubiquitin chain-induced p62 phase separation drives autophagic cargo segregation. *Cell Res.* **28**, 405–415
43. Strickfaden, H., Tolsma, T. O., Sharma, A., Underhill, D. A., Hansen, J. C., and Hendzel, M. J. (2020) Condensed chromatin behaves like a solid on the mesoscale *in vitro* and in living cells. *Cell* **183**, 1772–1784.e13
44. Frey, S., and Gorlich, D. (2007) A saturated FG-repeat hydrogel can reproduce the permeability properties of nuclear pore complexes. *Cell* **130**, 512–523
45. Frey, S., and Gorlich, D. (2009) FG/FxFG as well as GLFG repeats form a selective permeability barrier with self-healing properties. *EMBO J.* **28**, 2554–2567
46. Schmidt, H. B., and Gorlich, D. (2015) Nup98 FG domains from diverse species spontaneously phase-separate into particles with nuclear pore-like permselectivity. *Elife* **4**, e04251
47. Frey, S., Rees, R., Schunemann, J., Ng, S. C., Funfgeld, K., Huyton, T., and Gorlich, D. (2018) Surface properties determining passage rates of proteins through nuclear pores. *Cell* **174**, 202–217.e9
48. Wheeler, J. R., Matheny, T., Jain, S., Abrisch, R., and Parker, R. (2016) Distinct stages in stress granule assembly and disassembly. *Elife* **5**, e18413
49. Jain, S., Wheeler, J. R., Walters, R. W., Agrawal, A., Barsic, A., and Parker, R. (2016) ATPase-modulated stress granules contain a diverse proteome and substructure. *Cell* **164**, 487–498
50. Brangwynne, C. P., Eckmann, C. R., Courson, D. S., Rybarska, A., Hoege, C., Gharakhani, J., Julicher, F., and Hyman, A. A. (2009) Germline P granules are liquid droplets that localize by controlled dissolution/condensation. *Science* **324**, 1729–1732
51. Gibson, B. A., Doolittle, L. K., Schneider, M. W. G., Jensen, L. E., Gamarra, N., Henry, L., Gerlich, D. W., Redding, S., and Rosen, M. K. (2019) Organization of chromatin by intrinsic and regulated phase separation. *Cell* **179**, 470–484.e21
52. Shin, Y., Chang, Y. C., Lee, D. S. W., Berry, J., Sanders, D. W., Ronceray, P., Wingreen, N. S., Haataja, M., and Brangwynne, C. P. (2018) Liquid nuclear condensates mechanically sense and restructure the genome. *Cell* **175**, 1481–1491.e13
53. Nava, M. M., Miroshnikova, Y. A., Biggs, L. C., Whitefield, D. B., Metge, F., Boucas, J., Vihinen, H., Jokitalo, E., Li, X., Garcia Arcos, J. M., Hoffmann, B., Merkel, R., Niessen, C. M., Dahl, K. N., and Wickstrom, S. A. (2020) Heterochromatin-driven nuclear softening protects the genome against mechanical stress-induced damage. *Cell* **181**, 800–817.e22
54. Brangwynne, C. P., Mitchison, T. J., and Hyman, A. A. (2011) Active liquid-like behavior of nucleoli determines their size and shape in Xenopus laevis oocytes. *Proc. Natl. Acad. Sci. U. S. A.* **108**, 4334–4339
55. Zhang, H., Elbaum-Garfinkle, S., Langdon, E. M., Taylor, N., Occhipinti, P., Bridges, A. A., Brangwynne, C. P., and Gladfelter, A. S. (2015) RNA controls polyQ protein phase transitions. *Mol. Cell* **60**, 220–230
56. Elbaum-Garfinkle, S., Kim, Y., Szczepaniak, K., Chen, C. C., Eckmann, C. R., Myong, S., and Brangwynne, C. P. (2015) The disordered P granule protein LAF-1 drives phase separation into droplets with tunable viscosity and dynamics. *Proc. Natl. Acad. Sci. U. S. A.* **112**, 7189–7194
57. Feric, M., Vaidya, N., Harmon, T. S., Mitrea, D. M., Zhu, L., Richardson, T. M., Kriwacki, R. W., Pappu, R. V., and Brangwynne, C. P. (2016) Coexisting liquid phases underlie nucleolar subcompartments. *Cell* **165**, 1686–1697
58. Weirich, K. L., Banerjee, S., Dasbiswas, K., Witten, T. A., Vaikuntanathan, S., and Gardel, M. L. (2017) Liquid behavior of cross-linked actin bundles. *Proc. Natl. Acad. Sci. U. S. A.* **114**, 2131–2136
59. Agudo-Canalejo, J., Schultz, S. W., Chino, H., Migliano, S. M., Saito, C., Koyama-Honda, I., Stenmark, H., Brech, A., May, A. I., Mizushima, N., and Knorr, R. L. (2021) Wetting regulates autophagy of phase-separated compartments and the cytosol. *Nature* **591**, 142–146
60. Zhu, L., Richardson, T. M., Wacheul, L., Wei, M. T., Feric, M., Whitney, G., Lafontaine, D. L. J., and Brangwynne, C. P. (2019) Controlling the material properties and rRNA processing function of the nucleolus using light. *Proc. Natl. Acad. Sci. U. S. A.* **116**, 17330–17335
61. Brangwynne, C. P. (2013) Phase transitions and size scaling of membrane-less organelles. *J. Cell Biol.* **203**, 875–881
62. Voorhees, P. W. (1992) Ostwald ripening of 2-phase mixtures. *Annu. Rev. Mater. Sci.* **22**, 197–215
63. Bressloff, P. C. (2020) Active suppression of ostwald ripening: Beyond mean-field theory. *Phys. Rev. E* **101**, 042804
64. Lee, D. S. W., Wingreen, N. S., and Brangwynne, C. P. (2021) Chromatin mechanics dictates subdiffusion and coarsening dynamics of embedded condensates. *Nat. Phys.* **17**, 531–538
65. Berry, J., Weber, S. C., Vaidya, N., Haataja, M., and Brangwynne, C. P. (2015) RNA transcription modulates phase transition-driven nuclear body assembly. *Proc. Natl. Acad. Sci. U. S. A.* **112**, E5237–E5245
66. Zwicker, D., Hyman, A. A., and Julicher, F. (2015) Suppression of ostwald ripening in active emulsions. *Phys. Rev. E* **92**, 012317
67. Folkmann, A. W., Putnam, A., Lee, C. F., and Seydoux, G. (2021) Regulation of biomolecular condensates by interfacial protein clusters. *Science* **373**, 1218–1224
68. Wu, M., Xu, G., Han, C., Luan, P. F., Xing, Y. H., Nan, F., Yang, L. Z., Huang, Y., Yang, Z. H., Shan, L., Yang, L., Liu, J., and Chen, L. L. (2021) lncRNA SLERT controls phase separation of FC/DFCs to facilitate Pol I transcription. *Science* **373**, 547–555
69. Yamasaki, A., Alam, J. M., Noshiro, D., Hirata, E., Fujioka, Y., Suzuki, K., Ohsumi, Y., and Noda, N. N. (2020) Liquidity is a critical determinant for selective autophagy of protein condensates. *Mol. Cell* **77**, 1163–1175.e9
70. Wu, X., Ganzella, M., Zhou, J., Zhu, S., Jahn, R., and Zhang, M. (2021) Vesicle tethering on the surface of phase-separated active zone condensates. *Mol. Cell* **81**, 13–24.e7
71. Milovanovic, D., Wu, Y., Bian, X., and De Camilli, P. (2018) A liquid phase of synapsin and lipid vesicles. *Science* **361**, 604–607
72. Ma, W., and Mayr, C. (2018) A membraneless organelle associated with the endoplasmic reticulum enables 3'UTR-mediated protein-protein interactions. *Cell* **175**, 1492–1506.e19
73. Wan, G., Fields, B. D., Spracklin, G., Shukla, A., Phillips, C. M., and Kennedy, S. (2018) Spatiotemporal regulation of liquid-like condensates in epigenetic inheritance. *Nature* **557**, 679–683
74. Zhao, Y. G., and Zhang, H. (2020) Phase separation in membrane biology: The interplay between membrane-bound organelles and membraneless condensates. *Dev. Cell* **55**, 30–44
75. Prinz, W. A., Toulmay, A., and Balla, T. (2020) The functional universe of membrane contact sites. *Nat. Rev. Mol. Cell Biol.* **21**, 7–24
76. Delarue, M., Brittingham, G. P., Pfeffer, S., Surovtsev, I. V., Pinglay, S., Kennedy, K. J., Schaffer, M., Gutierrez, J. I., Sang, D., Poterewicz, G., Chung, J. K., Plitzko, J. M., Groves, J. T., Jacobs-Wagner, C., Engel, B. D., *et al.* (2018) mTORC1 controls phase separation and the biophysical properties of the cytoplasm by tuning crowding. *Cell* **174**, 338–349.e20

77. Shen, Y., Ruggeri, F. S., Vigolo, D., Kamada, A., Qamar, S., Levin, A., Iserman, C., Alberti, S., George-Hyslop, P. S., and Knowles, T. P. J. (2020) Biomolecular condensates undergo a generic shear-mediated liquid-to-solid transition. *Nat. Nanotechnol.* **15**, 841–847
78. Riback, J. A., Katanski, C. D., Kear-Scott, J. L., Pilipenko, E. V., Rojek, A. E., Sosnick, T. R., and Drummond, D. A. (2017) Stress-triggered phase separation is an adaptive, evolutionarily tuned response. *Cell* **168**, 1028–1040.e19
79. Franzmann, T. M., Jahnel, M., Pozniakovsky, A., Mahamid, J., Holehouse, A. S., Nüske, E., Richter, D., Baumeister, W., Grill, S. W., Pappu, R. V., Hyman, A. A., and Alberti, S. (2018) Phase separation of a yeast prion protein promotes cellular fitness. *Science* **359**, eaao5654
80. Jung, J. H., Barbosa, A. D., Hutin, S., Kumita, J. R., Gao, M. J., Derwort, D., Silva, C. S., Lai, X. L., Pierre, E., Geng, F., Kim, S. B., Baek, S., Zubieta, C., Jaeger, K. E., and Wigge, P. A. (2020) A prion-like domain in ELF3 functions as a thermosensor in Arabidopsis. *Nature* **585**, 256–260
81. Heim, M., Keerl, D., and Scheibel, T. (2009) Spider silk: From soluble protein to extraordinary fiber. *Angew. Chem. Int. Ed. Engl.* **48**, 3584–3596
82. Jin, H. J., and Kaplan, D. L. (2003) Mechanism of silk processing in insects and spiders. *Nature* **424**, 1057–1061
83. Zhang, Y., Narlikar, G. J., and Kutateladze, T. G. (2021) Enzymatic reactions inside biological condensates. *J. Mol. Biol.* **433**, 166624
84. Kuznetsova, I. M., Zaslavsky, B. Y., Breydo, L., Turoverov, K. K., and Uversky, V. N. (2015) Beyond the excluded volume effects: Mechanistic complexity of the crowded milieu. *Molecules* **20**, 1377–1409
85. Wang, Z., Zhang, G., and Zhang, H. (2019) Protocol for analyzing protein liquid-liquid phase separation. *Biophys. Rep.* **5**, 1–9
86. Taylor, N. O., Wei, M. T., Stone, H. A., and Brangwynne, C. P. (2019) Quantifying dynamics in phase-separated condensates using fluorescence recovery after photobleaching. *Biophys. J.* **117**, 1285–1300
87. Kroschwald, S., Maharana, S., Mateju, D., Malinovska, L., Nuske, E., Poser, I., Richter, D., and Alberti, S. (2015) Promiscuous interactions and protein disaggregases determine the material state of stress-inducible RNP granules. *Elife* **4**, e06807
88. Nott, T. J., Petsalaki, E., Farber, P., Jervis, D., Fussner, E., Plochowietz, A., Craggs, T. D., Bazett-Jones, D. P., Pawson, T., Forman-Kay, J. D., and Baldwin, A. J. (2015) Phase transition of a disordered nuage protein generates environmentally responsive membraneless organelles. *Mol. Cell* **57**, 936–947
89. Lin, Y., Mori, E., Kato, M., Xiang, S., Wu, L., Kwon, I., and McKnight, S. L. (2016) Toxic PR poly-dipeptides encoded by the C9orf72 repeat expansion target LC domain polymers. *Cell* **167**, 789–802.e12
90. Feng, Z., Chen, X., Wu, X., and Zhang, M. (2019) Formation of biological condensates *via* phase separation: Characteristics, analytical methods, and physiological implications. *J. Biol. Chem.* **294**, 14823–14835
91. Liu, Z., Yang, Y., Gu, A., Xu, J., Mao, Y., Lu, H., Hu, W., Lei, Q. Y., Li, Z., Zhang, M., Cai, Y., and Wen, W. (2020) Par complex cluster formation mediated by phase separation. *Nat. Commun.* **11**, 2266
92. Chen, D., Wang, Z., Zhao, Y. G., Zheng, H., Zhao, H., Liu, N., and Zhang, H. (2020) Inositol polyphosphate multikinase inhibits liquid-liquid phase separation of TFEB to negatively regulate autophagy activity. *Dev. Cell* **55**, 588–602.e7
93. Ryan, V. H., Dignon, G. L., Zerze, G. H., Chabata, C. V., Silva, R., Conicella, A. E., Amaya, J., Burke, K. A., Mittal, J., and Fawzi, N. L. (2018) Mechanistic view of hnRNPA2 low-complexity domain structure, interactions, and phase separation altered by mutation and arginine methylation. *Mol. Cell* **69**, 465–479.e7
94. Qamar, S., Wang, G. Z., Randle, S. J., Ruggeri, F. S., Varela, J. A., Lin, J. Q., Phillips, E. C., Miyashita, A., Williams, D., Strohl, F., Meadows, W., Ferry, R., Dardov, V. J., Tartaglia, G. G., Farrer, L. A., *et al.* (2018) FUS phase separation is modulated by a molecular chaperone and methylation of arginine cation-pi interactions. *Cell* **173**, 720–734.e15
95. Singatulina, A. S., Hamon, L., Sukhanova, M. V., Desforges, B., Joshi, V., Bouhss, A., Lavrik, O. I., and Paste, D. (2019) PARP-1 activation directs FUS to DNA damage sites to form PARG-reversible compartments enriched in damaged DNA. *Cell Rep.* **27**, 1809–1821.e5
96. Boyko, S., Surewicz, K., and Surewicz, W. K. (2020) Regulatory mechanisms of tau protein fibrillation under the conditions of liquid-liquid phase separation. *Proc. Natl. Acad. Sci. U. S. A.* **117**, 31882–31890
97. Drelich, J., Fang, C., and White, C. L. (2002) Measurement of interfacial tension in fluid-fluid systems. *Encycl. Surf. Colloid Sci.* **3**, 3152–3166
98. Lyu, X. C., Wang, J., Wang, J. Q., Yin, Y. S., Zhu, Y., Li, L. L., Huang, S. R., Peng, S., Xue, B. X., Liao, R. Y., Wang, S. Q., Long, M. A., Wohland, T., Chua, B. T., Sun, Y. J., *et al.* (2021) A gel-like condensation of Cidec generates lipid-permeable plates for lipid droplet fusion. *Dev. Cell* **56**, 2592–2606.e7
99. Wang, J., Choi, J. M., Holehouse, A. S., Lee, H. O., Zhang, X. J., Jahnel, M., Maharana, S., Lemaitre, R., Pozniakovsky, A., Drechsel, D., Poser, I., Pappu, R. V., Alberti, S., and Hyman, A. A. (2018) A molecular grammar governing the driving forces for phase separation of prion-like RNA binding proteins. *Cell* **174**, 688–699.e16
100. Gui, X., Luo, F., Li, Y., Zhou, H., Qin, Z., Liu, Z., Gu, J., Xie, M., Zhao, K., Dai, B., Shin, W. S., He, J., He, L., Jiang, L., Zhao, M., *et al.* (2019) Structural basis for reversible amyloids of hnRNPA1 elucidates their role in stress granule assembly. *Nat. Commun.* **10**, 2006
101. Kaur, T., Alshareedah, I., Wang, W., Ngo, J., Moosa, M. M., and Banerjee, P. R. (2019) Molecular crowding tunes material states of ribonucleoprotein condensates. *Biomolecules* **9**, 71
102. Alshareedah, I., Kaur, T., Ngo, J., Seppala, H., Kounatse, L. A. D., Wang, W., Moosa, M. M., and Banerjee, P. R. (2019) Interplay between short-range attraction and long-range repulsion controls reentrant liquid condensation of ribonucleoprotein-RNA complexes. *J. Am. Chem. Soc.* **141**, 14593–14602
103. Jawerth, L. M., Ijavi, M., Ruer, M., Saha, S., Jahnel, M., Hyman, A. A., Julicher, F., and Fischer-Friedrich, E. (2018) Salt-dependent rheology and surface tension of protein condensates using optical traps. *Phys. Rev. Lett.* **121**, 258101
104. Wei, M. T., Elbaum-Garfinkle, S., Holehouse, A. S., Chen, C. C., Feric, M., Arnold, C. B., Priestley, R. D., Pappu, R. V., and Brangwynne, C. P. (2017) Phase behaviour of disordered proteins underlying low density and high permeability of liquid organelles. *Nat. Chem.* **9**, 1118–1125
105. Pan, Q., Sun, D., Xue, J., Hao, J., Zhao, H., Lin, X., Yu, L., and He, Y. (2021) Real-time study of protein phase separation with spatiotemporal analysis of single-nanoparticle trajectories. *ACS Nano* **15**, 539–549
106. Kihara, T., Ito, J., and Miyake, J. (2013) Measurement of biomolecular diffusion in extracellular matrix condensed by fibroblasts using fluorescence correlation spectroscopy. *PLoS One* **8**, e82382
107. Peng, S. J., Li, W. P., Yao, Y. R., Xing, W. J., Li, P. L., and Chen, C. L. (2020) Phase separation at the nanoscale quantified by dcFCCS. *Proc. Natl. Acad. Sci. U. S. A.* **117**, 27124–27131
108. Chong, S. S., Dugast-Darzacq, C., Liu, Z., Dong, P., Dailey, G. M., Cattoglio, C., Heckert, A., Banala, S., Lavis, L., Darzacq, X., and Tjian, R. (2018) Imaging dynamic and selective low-complexity domain interactions that control gene transcription. *Science* **361**, eaar2555
109. Beutel, O., Maraspini, R., Pombo-Garcia, K., Martin-Lemaitre, C., and Honigmann, A. (2019) Phase separation of zonula occludens proteins drives formation of tight junctions. *Cell* **179**, 923–936.e11
110. Whitesides, G. M. (2006) The origins and the future of microfluidics. *Nature* **442**, 368–373
111. Sackmann, E. K., Fulton, A. L., and Beebe, D. J. (2014) The present and future role of microfluidics in biomedical research. *Nature* **13**, 181–189
112. Linsenmeier, M., Kopp, M. R. G., Stavrakis, S., de Mello, A., and Arosio, P. (2021) Analysis of biomolecular condensates and protein phase separation with microfluidic technology. *Biochim. Biophys. Acta Mol. Cell Res.* **1868**, 118823
113. Taylor, N., Elbaum-Garfinkle, S., Vaidya, N., Zhang, H., Stone, H. A., and Brangwynne, C. P. (2016) Biophysical characterization of organelle-based RNA/protein liquid phases using microfluidics. *Soft Matter* **12**, 9142–9150
114. Bremer, A., Mittag, T., and Heymann, M. (2020) Microfluidic characterization of macromolecular liquid-liquid phase separation. *Lab. Chip* **20**, 4225–4234
115. Kroschwald, S., and Alberti, S. (2017) Gel or die: Phase separation as a survival strategy. *Cell* **168**, 947–948
116. Gwon, Y., Maxwell, B. A., Kolaitis, R. M., Zhang, P., Kim, H. J., and Taylor, J. P. (2021) Ubiquitination of G3BP1 mediates stress granule disassembly in a context-specific manner. *Science* **372**, eabf6548